

# Prediction of Soil Hydrological Responses under Landuse/Cover Changes using Markov Chains in Jiroft Watershed, Iran

#### ARTICLEINFO

#### Article Type Original Research

#### Authors

Neda Najafi Kalyani, *Ph.D.*<sup>1</sup> Abolfazl Ranjbar Fordoei, *Ph.D.*<sup>2\*</sup> Fateme Panahi, *Ph.D.*<sup>3</sup> Hojat Musavi, *Ph.D.*<sup>3</sup>

#### How to cite this article

Najafi Kalyan N., Ranjbar Fordoei A., Panahi F., Musavi H. Prediction of Soil Hydrological Responses under Land-use/Cover Changes using Markov Chains in Jiroft Watershed, Iran. ECOPERSIA 2022; 10(1): 47-59.

#### DOR:

20.1001.1.23222700.2022.10.1.5.8

Resources and Earth Science, University of Kashan, Kashan, Iran.

<sup>2</sup>Professor, Faculty of Natural
Resources and Earth Science,
University of Kashan, Kashan
8731753153, Iran.

<sup>3</sup>Assistant Professor, Faculty of Natural
Resources and Earth Science,

University of Kashan, Kashan, Iran

<sup>1</sup>Ph.D. student, Faculty of Natural

#### \* Correspondence

Address: Faculty of Natural Resources and Earth Science, University of Kashan, Kashan 8731753153, Iran.
Tel: 03155913224
Cell No: 09132841182
Fax: 03155914999
Email: aranjbar@kashanu.ac.ir

#### Article History

Received: July 28, 2021 Accepted: October 6, 2021 Published: December 23, 2021

#### ABSTRACT

Aims: This study aims to evaluate the Soil Hydrological Response (SHR) under land-use/land-cover (LU/LC) (current management/current land cover) using a field-oriented and remote sensing database in the Jiroft watershed, Iran.

Materials & Methods: Land-use maps were extracted from Landsat images using the supervised classification method for 1987-2017. The results were validated against the field data from 100 points, where we found the Kapp index to be greater than 80%, indicating an acceptable accuracy in land-use classification. The LU/LC map was then projected for 2047 using the CA-Markov model. The Curve Number (CN) for each land-use was determined from superimposing LU/LC and the soil hydrological group map. The Soil Conservation Services-Curve Number method (SCS-CN) was employed to estimate runoff.

**Findings:** Rangelands with good (densely vegetated) and moderate vegetation conditions had a decreasing trend in terms of area (i.e., -2.94% and -3.64% in 1987- 2017), while croplands, orchards, residential, and saline areas had an increasing trend (by 1.46%, 0.88%, 0.33%, and 7.21%). We found that agricultural lands, saline lands, and residential areas will increase by 0.75, 5.5, and 0.13% by 2047, respectively. The highest Curve Number (CN) values were detected in desert lands, residential areas, and poor-condition rangelands with the respective values of 88, 88.67, and 84.67. As for 2047, residential areas, deserts, and rangelands with poor conditions with the respective CN values of 89, 88, and 84.67 would contribute substantially to runoff generation. **Conclusion:** We found a considerable increase (up to 6 mm increase) in runoff depth in some land-uses and more than 3.4% increase in the area of the high runoff producing class (IV). We believe that higher runoff production potential and more intense and short rain showers should be considered seriously in terms of possible flash floods in the future.

Keywords: curve number; land-use change; Markov model; remote sensing; soil conservation services.

### CITATION LINKS

[1] Jayasree V., Venkatesh B. Evaluating the ... [2] Zhang F., Tiyip T., Feng Z., Kung H.T., Johnson V., Ding J., Tashpolat N., Sawut M., Gui D. Spatio-temporal... [3] Baker T.J., Miller S.N. Using the...[4] de Oliveira Barros K., Ribeiro... [5] Yang X., Ren L., Liu Y., Jiao D., Jiang S. Hydrological... [6] Romulus C., Iulia F., Ema C. Assessment of surface runoff depth changes in Sărățel River basin, Romania... [7] Scheffler R., Neill C., Krusche A.V., Elsenbeer H. Soil hydraulic response to... [8] Ladisa G., Todorovic M., Liuzzi G.T. A GIS-based approach... [9] Wijitkosum S. The impact of land use and spatial changes on... [10] Yousefi M., Mikaniki J., Ashrafi A., Neysani Samani N. Land-use... [11] Ranzi R., Le T.H., Rulli M.C. A RUSLE approach to... [12] Huang T.C., Lo K.F.A. Effects of land-use change on sediment and... [13] Hong N.M., Chu H. J., Lin Y. P., Deng D. P. Effects of land cover changes induced by large... [14] Halder A., Ghosh A., Ghosh S. Supervised and unsupervised landuse map generation from remotely sensed images using ant based systems. Appl. Soft Comput. 2011;11(8):5770-5781. [15] Veldkamp A., Lambin E.F. Predicting... [16] Keshtkar H., Voigt W. A spatiotemporal analysis of landscape change using an... [17] Rimal B., Zhang L., Keshtkar H., Haack B.N., Rijal S., Zhang P. Land use/land cover...[18] Torrens P.M., O'Sullivan D. Cellular... [19] Ding H.p., Chen J.p., Wang G.w., editors. A model for... [20] Ghaderi S., Zare Chahouki M., Azarnivand H., Tavili A., Raygani B. Land-use Change... [21] Yousefi S., Mirzaee S., Tazeh M., Pourghasemi... [22] Firozjaei M.K., Kiavarz M., Alavipanah S.K., Lakes... [23] Cronshey R., Roberts R., Miller N., editors. Urban hydrology... [24] Satheeshkumar S., Venkateswaran S., Kannan R. Rainfall-runoff estimation... [25] Naboureh A., Moghaddam M.H.R., Feizizadeh B., Blaschke T. An integrated object-based image... [26] Mosayebi M., Maleki M. Change detection in land use using... [27] Salehi N., Ekhtesasi M.R., Talebi A. Predicting locational... [28] Jafari Shalamzari M., Zhang W., Gholami A., Zhang Z. Runoff Harvesting Site... [29] Sheikh V.B., Jafari Shalamzari M., Farajollahi A., Fazli P. Soil erosion under ... [30] Hu S., Fan Y., Zhang T. Assessing the effect of land-use change...[31] Ngo T.S., Nguyen D.B., Rajendra P.S. Effect of land-use change on runoff and sediment yield in Da River Basin of Hoa Binh province, Northwest...

#### Introduction

The effect of land-use/cover change (LU/LC) on land hydrological processes is a global concern and a great challenge for researchers and policymakers <sup>[1]</sup>. Understanding how changes in land-use/cover influence the soil hydrological response (SHR) would significantly improve the land dynamics predictability for land management, especially in terms of flood prevention, sustainable land-use management, and vegetation cover management <sup>[2]</sup>.

Generally, land cover changes due to environmental and anthropogenic factors can alter SHR <sup>[3]</sup>. Although LU/LC changes may occur in all climatic areas (e.g., arid, semi-arid, or sub-humid regions), arid lands, due to their fragile environmental conditions, under-developed soils, and sparse vegetation, are more prone to excessive runoff production <sup>[4]</sup>.

Due to the susceptibility of arid soils to erosion, SHR may be rapidly altered due to vegetation changes <sup>[1,5]</sup>. In particular, floods, as the most recurrent natural hazards with irrecoverable socio-economic and human losses <sup>[6]</sup>, occur in response to the changes in land cover and SHR <sup>[7]</sup>. Therefore, evaluating the relationship between LU/LC changes and SHR can improve sustainable land management.

SHR can be evaluated using direct observation/measurements, mathematical models, parametric equations, and remote sensing techniques [8, 9]. Nowadays, models are accurate, fast, and cost-effective for assessing environmental changes [10]. A wide range of models have been developed for SHR evaluation, with various degrees of freedom in complexity, embodied processes, and the data required for calibration and utilization [11].

Generally, evaluation of SHR under changing conditions requires models that can simulate flow regimes under different scenarios <sup>[12]</sup>. However, contradictory results have been reported on the impact of land-use/cover on SHR over different spatiotemporal scales <sup>[1,13]</sup>. Therefore, SHR changes are case-specific and require local and regional studies to determine their range and mechanisms.

As mentioned earlier, SHR is highly dependent on LU/LC. There are several models available to classify land-use and cover using remote sensing (RS) techniques and geographic information systems (GIS), including but not limited to the supervised and unsupervised classification techniques [14]. Remote sensing and GIS are indispensable tools for application in arid areas characterized by data scarcity and difficulty of access. With the advent of more sophisticated models, it is now possible to evaluate former and current land cover and uses and project it onto and foreseeable future [15]. The chief amongst these models is the Markov Chain model, which calculates future changes based on past events [16, 17]. In addition to Markov Chain models, another set of tools, called Cellular Automata, have been developed for evaluating the interrelationships between adjacent land-uses [18]. The Markov Chain Models and the Cellular Automata combination provide researchers with an almost perfect tool for identifying and projecting different land-use/ covers under different circumstances [4]. The results of these methods are simply verifiable using field works and satellite images [4].

The impact of LU/LC on SHR is then simply achievable by applying the CA-Markov method. We adopted this method since it is a reliable means of predicting the changes in SHR in the future based on its changes over time and space [4,17,19-21]. Most of these studies are restricted in either time or space domains, and therefore studies with broader domains, such as this study, are required. Therefore, the main objective of this study is to investigate possible changes of SHR under LU/

LC over 1987-2017 in the Jiroft watershed of Iran. The study area is located in Kerman Province of Iran, with a long history of flash floods, and is seriously suffering from data unavailability and remoteness. Therefore, the application of RS and GIS methods in the form of CA-Markov to evaluate SHR changes over time and space can remarkably aid land managers in better allocating resources and to avoid possible flash floods or even nourish the already diminished

3ed water resources of the area. The study will cover the period of 1987 – 2017, and we will be using the CA-Markov method to predict land-use changes by the year 2047 to see how the business-as-usual scenario could affect SHR in the area. We believe that future changes will favor more runoff production and hence the likelihood of flash floods in the study area.

# Materials & Methods Study area

The study area of our research is the Jiroft Watershed, located in the Kerman Province of Iran. The main city of the area is Kahnouj, and the rest of the population centers are in the form of dispersed villages. The studied region extends for about 10,258 km<sup>2</sup> and lies between the latitudes of 27°34′30.1″ to 28°46'25.5" N and the longitudes of 57°35′26.7" to 58°55′32.1" E, in central Iran (Figure 1). The region has an annual rainfall of 150 mm and an average annual temperature of 15.4 °C. The area's average height is 574 m above sea level, ranging from 359 m to 3549 m. The diverse topography, together with rainfall variability, creates different geomorphological facies (Table 3). Different land-uses are evident in the area, including agricultural lands, orchards, rangelands, and residential areas. The vegetation composition of the area is dominated by species like Juniperus exelsa Acacia sejal, Amygdalus scoparia, Tamarix articulata, Zygophyllum atriplicoides,

and Acer cinerascens. High temperatures and low rainfall are the main climatic characteristics of the area. However, flash floods occur intermittently (direct observations) and cost considerable damage to the properties and infrastructure and therefore, assessing the dynamics of land-use changes and their impact on flooding is of great importance.

### **Data compilation**

A setup of three stages was developed to perform this study: 1) Extracting LU/LC maps from satellite images, 2) assessing LU/LC and modeling the SHR during 1987-2017, and 3) projecting LU/LC and modeling the SHR for 2017-2047.

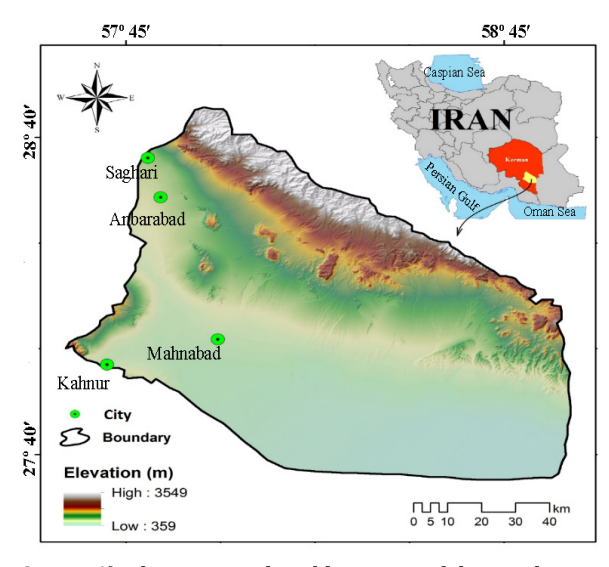


**Figure 1)** The geographical location of the study area in Kerman province in Iran.

# Land-use/cover changes

Satellite images of Thematic Mapper (TM) and Operational Land Imager (OLI) sensors of Landsat satellite related to three periods of 1987, 2002 (as the mid-point), and 2017 were used to evaluate land-use changes in the region (Table 1). All the analyses were performed in the Erdas Imagine 15.0 and ArcGIS 10.3.

The obtained images (from https://earthexplorer.usgs.gov/ database) were geometrically corrected (quadratic transforms) and projected to the World Geodetic System (WGS-1984). The Fast Line-of-sight Atmo-

spheric Analysis of Hypercubes (FLAASH) model was used for the atmospheric correction of all Landsat images. The Histogram Equalization technique was used to adjust the sensor's digital data <sup>[22]</sup>. We used the supervised Maximum Likelihood Estimation for land-use classifications. The results were then validated against ground data (100 points randomly distributed across the study area) and google earth images. The Kappa index was used to evaluate the generated maps accuracy <sup>[23]</sup> as (Eq. 1):

$$Kappa = \frac{P_0 - P_c}{1 - P_c} \times 100$$
 Eq. (1)

where is the observed and is the expected conformity.

### Projecting LU/LC for the future

To project land-use classes, the CA-Markov was performed in the IDRISI Terrset software. For this aim, LU/LC maps of 1987 and 2002 were used to simulate 2017 maps. The land-use map of 2017 was validated against the actual land-use map of the study area using the Kappa index.

### Calculating surface runoff

We first obtained the geology and vegetation cover maps at the scale of 1:100000 from the Department of Natural Resources, Watershed Management Office of Jiroft. The NASA Shuttle Radar Topographic Mission (SRTM) map prepared the topography and slope direction maps. Then the working unit map was prepared by overlaying geology, slope direction, topography, and vegetation cover maps in the GIS environment.

Soils were classified according to the Natural Resource Conservation Service into four Hydrologic Soil Groups based on the 'oil's runoff potential. The four Hydrologic Groups are A, B, C, and D. Where group A generally has the smallest runoff potential, and group D has the greatest potential. Soil hydrological groups were defined based on soil texture (obtained from the 1:100000 soil map of the area from the depart-

ment of natural resources) and the standard tables suggested by Cronshey *et al.* <sup>[24]</sup> and the United States Department of Agriculture <sup>[25]</sup>. Climate data was acquired from the Jiroft meteorological station. The Penman-Monteith method <sup>[26]</sup> was used to estimate the potential Evapotranspiration (ET):

$$E_T = \frac{\Delta R_n + (e_a - e_d) * \frac{\rho * c_p}{r_a}}{\lambda (\Delta + \gamma * (1 + \frac{r_s}{r_a}))}$$
Eq. (2)

Where is the net radiation (W.m $^{-2}$ ), is the density of air, is the specific heat of air,  $r_s$  is the net resistance to diffusion through surfaces of leaves and soil (s.m $^{-1}$ ),  $r_a$  is the net resistance to diffusion through the air from surfaces to the height of the measuring instruments (s.m $^{-1}$ ), is the hydrometric constant, is de.dT $^{-1}$ ,  $e_a$  is the saturated vapor pressure at air temperature and  $e_d$  is the mean vapor pressure. ET is the total quantity of water vapor entering the atmosphere through evapotranspiration from surfaces or the leaves of plants. The annual rainfall surplus was calculated as the difference between precipitation and ET.

### **Surface Runoff Generation**

The SCS-CN method was used for rainfall-runoff evaluations [27]. We used the data on a) land cover in years 1987, 2002, and 2017 b) rainfall surplus (long term average), c) slope gradient, and d) soil texture to determine surface runoff depth. The surface runoff was calculated for the entire area in each period as Eq. 3.

$$R = \frac{(P - 0.2S)^2}{P + 0.8S}$$
 Eq. (3)

where R denotes the runoff (mm), P is the rainfall (mm), and S is the detention (mm) that is calculated by Eq. 4:

$$S = \frac{25400}{CN} - 254$$
 Eq. (4)

where CN is the curve number.

**Table 1**) The changes in the areal extent of land-use classes from 1987 to 2017.

T 1 /	1987		2002		2017	
Land-use/cover	Area (ha)	%	Area (ha)	%	Area (ha)	%
Open Canopy forests	6563.52	0.64	7652.74	0.75	8841.96	0.86
Good-condition rangelands	45419.49	4.43	35312.895	3.44	15306.30	1.49
Moderately-dense rangelands	363864.78	35.48	345176.55	33.67	326588.31	31.84
Poor-condition rangelands	491110.92	47.88	460655.18	44.93	450299.43	43.91
Shrubs and orchards	7715.34	0.75	14166.6	1.38	16717.86	1.63
Agricultural lands	62277.75	6.07	69693.79	6.80	77209.83	7.53
Residential areas	484.29	0.05	3140.69	0.31	3897.09	0.38
Saline lands	46809.27	4.56	85692.705	8.36	120676.14	11.77
Deserts	1372.05	0.13	3676.765	0.36	6081.48	0.59
Total	1025617.41	100.00	1025617.41	100.00	1025617.41	100.00

### **Findings**

The map of the geomorphological facies was prepared from field visits and verified on Google Earth 9.0 (Figure 2). In total, 34 facies were detected, which are provided in detail in Table 3. During the field visits, we noticed that the major facies (piedmont plains) had sparse vegetation and were marked with different water erosion types, testifying to the activity of severe water erosion in the area.

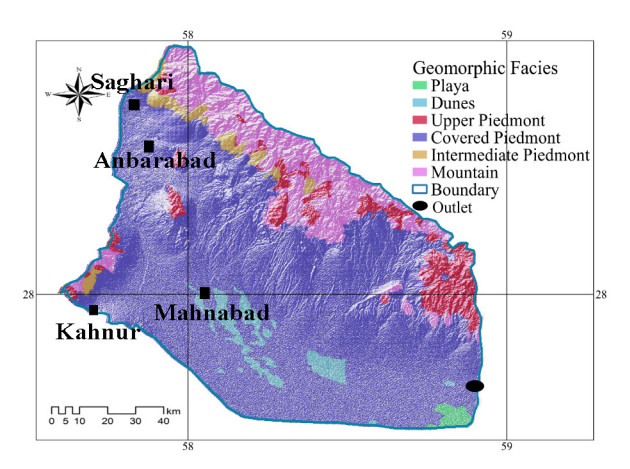


**Figure 2)** The major geomorphic facies of the area, a more detailed description of all minor geomorphic facies is provided in the table.

We also found that hydrological group C is the dominant group (59.57 %), followed by group D (22.21%) and group B (18.22% (the results are not brought in here). Based on the results, the kappa index and the overall accuracy of images used in different years were higher than 0.8. In particular, the kappa index for 1987, 2002, and 2017 were estimated to be 0.829, 0.86, and 0.91, respectively, which indicated a high accuracy [23, 28, 29]. In this regard, a LU/LC map with high reliability and accuracy (i.e., kappa coefficient of 0.72) in 2047 was obtained for the region (Table 2), as presented in Figure 3. Table 2 also provides the details of the commission and omission errors. Low error rates indicate the validity of land-use classifications. Table 1 provides detailed changes in the area of LU/LC classes in different years. Rangelands with poor and moderate vegetation conditions and saline lands are the dominant land-use types. According to Table 2, rangelands with good vegetation conditions shrunk remarkably in size be-

**Table 2)** Overall accuracy and kappa values for the target analyzing years.

Year	Kappa values	Overall accuracy	Commission Error	Omission Error
1987	0.829	0.87	15.00	15.07
2002	0.86	0.898	13.85	13.96
2017	0.91	0.915	7.75	7.87

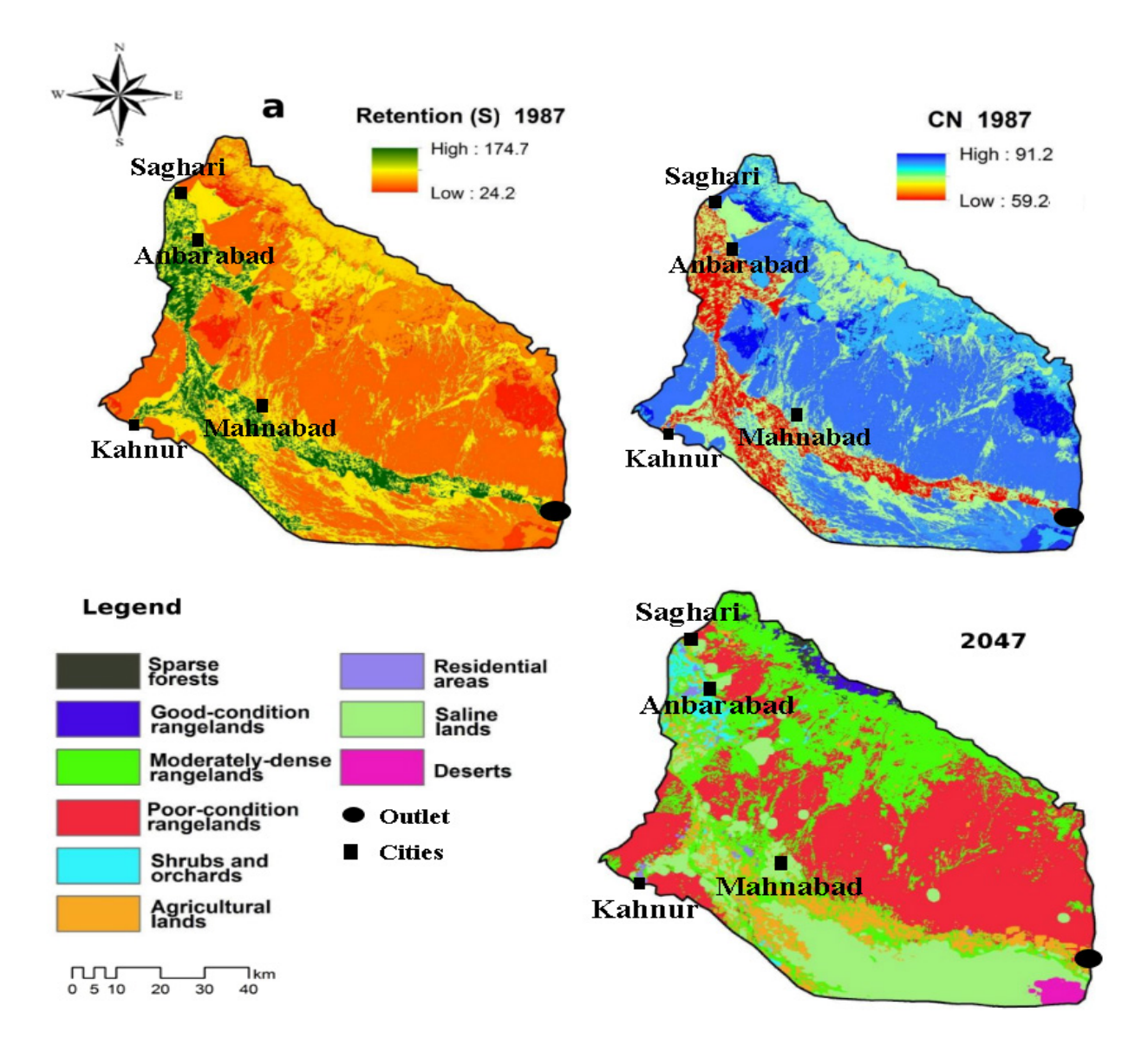


**Figure 3)** LU/LC of Jiroft region during 1987-2047.

tween 1987 and 2017. Orchards, agricultural lands, desert lands, and residential areas have expanded considerably (i.e., 1.46%, 0.88%, 0.33%, and 7.21% increase from

1987 to 2017). The interesting case is the saline lands which have tripled in size over the study time. Other land-use classes did not show a clear or important growth or shrink-

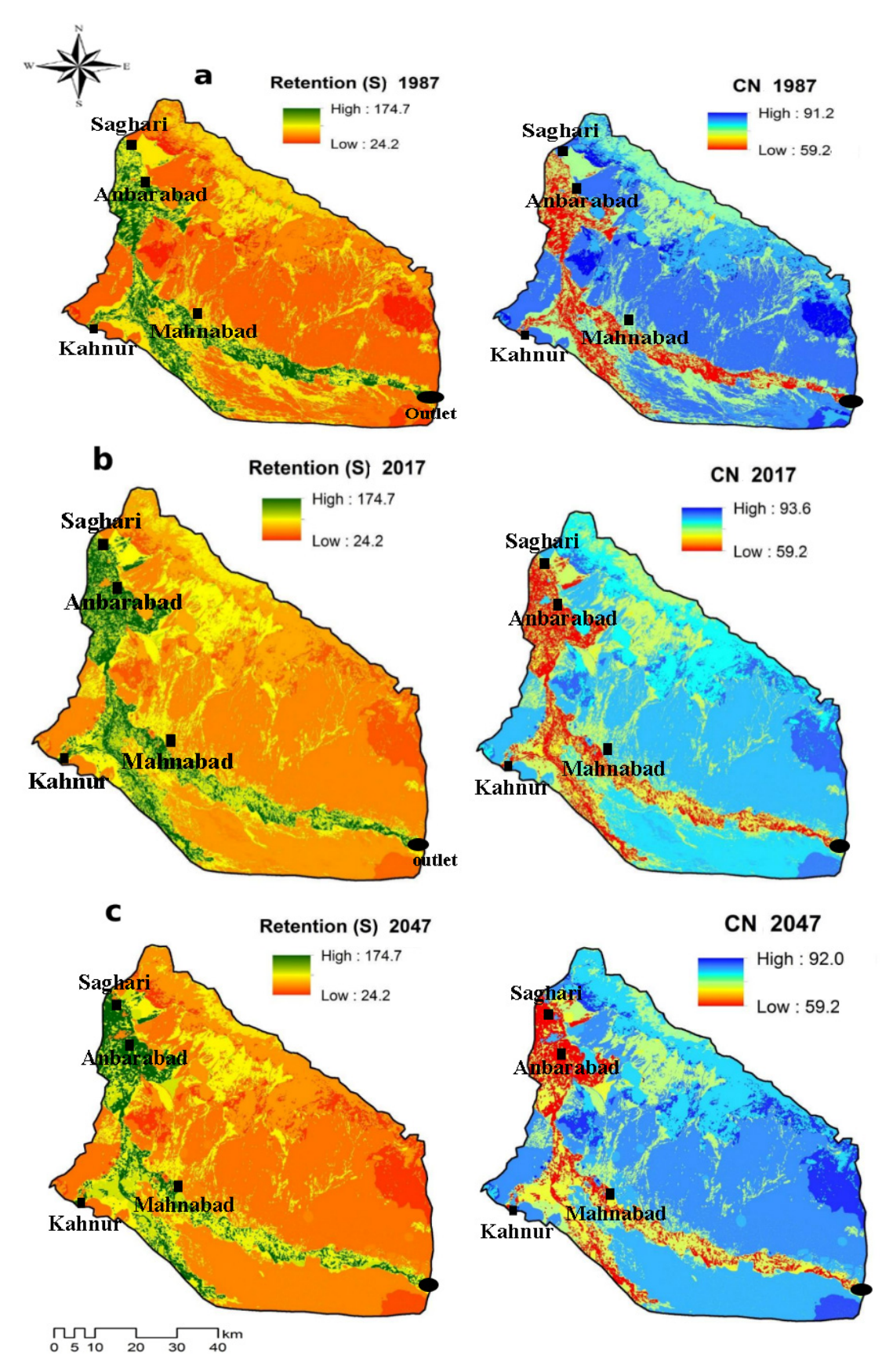


**Figure 4)** Spatial change in retention (S) and curve number (CN) values in the study area during 1987 (a), 2017 (b), and 2047 (c)

age in time. Figure 3 illustrates the changes in each land-use class during the studied period. In the northern part, the conversion of all land-use classes to good-condition rangelands and forests is discernible, while conversion to poor-condition rangelands is more evident from west to east. Most of the changes have occurred in saline lands and agricultural land use in the southern parts. A significant conversion to residential land use is also evident to the east.

### **Projected CN values**

The highest Curve Number (CN) values were detected in desert lands, residential areas, and poor-condition rangelands with the respective values of 88, 88.67, and 84.67. In 2017, the highest CN value belonged to the three abovementioned land-uses with the respective values of 88, 85, and 84.67. According to the projected land-use map for 2047, it seems that residential areas, deserts, and poor-condition rangelands with the respective CN values of 89, 88, and 84.67 will contribute substantially to runoff generation. In 1987, residential areas with the hydrological group-C had the highest CN value of 90.

In 2017, poor-condition rangelands with the hydrological group-D and a CN value of 89 increased significantly. Moreover, the projected LU/LC in 2047 indicates that residential areas with the hydrological groups D and C will have the highest CN values, which will lead to a significant increase in the region's flood potential (Figure 4).

### Projection of runoff generation potential

The runoff generation zones of 1987 and 2002 were obtained by superimposing soil hydrological groups and soil surface characteristic maps, and the results were extrapolated to 2047 (Figure 5). As it appears, the region's highest runoff generation is related to the poor-condition rangelands, which, with their sparse vegetation and lack of protective cover, could generate considerable amounts of runoff.

Table 3 provides a detailed description of the average changes in runoff generation potential in each geomorphological facies. Accordingly, in 2047, there will be significant growth in runoff production in poor-condition rangelands. However, other areas, such as agricultural lands, exhibited a reduction

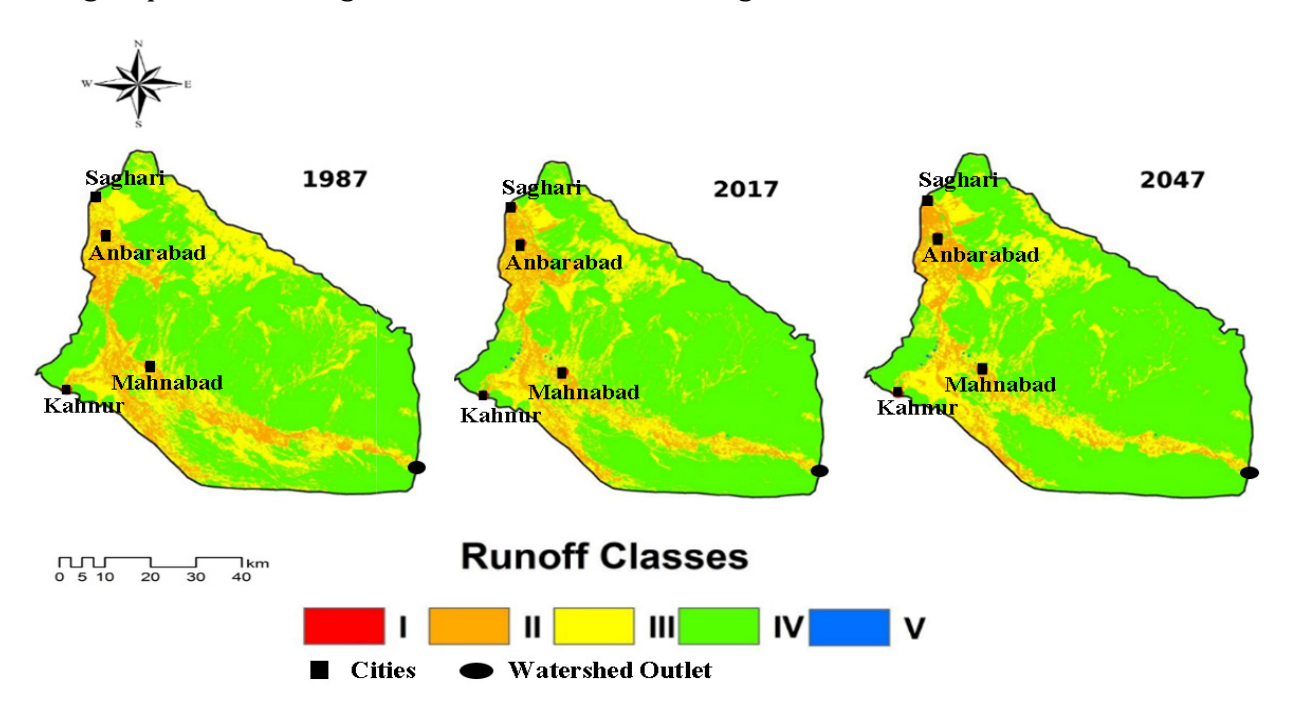


Figure 5) Spatial distribution of runoff classes in area in 1987, 2017 and 2047.

**Table 3)** Changes of average runoff (mm) in different geomorphological facies during 1987-2047.

Pasta	Runoff amount (mm)						
Facies	1987	2017	2047	1987-2017 (ΔR)	2017-2047 (ΔR)	1987-2047 (ΔR)	
Metamorphic granite mountains	89.16	90.39	92.49	1.23	2.10	3.33	
Granite hills	85.31	88.06	88.71	2.75	0.65	3.40	
Andesitic volcanic rock interlayers	85.66	88.24	88.48	2.58	0.24	2.81	
Gypsum marly filaments	107.23	108.68	108.89	1.45	0.21	1.66	
Relatively high Andesitic mountains	84.46	89	89.59	4.54	0.59	5.13	
Marly mountains	108.26	109.47	109.37	1.21	-0.1	1.11	
Planted dunes	87.17	90.53	92.30	3.36	1.76	5.12	
Sandy lands with rangeland cover	104.26	109.18	110.09	4.92	0.91	5.83	
Young alluvial fans (lowlands)	108.86	109.82	109.87	0.96	0.05	1.01	
Alluvial rivers	140.65	135.69	136.30	-4.96	0.61	-4.35	
Coarse-grained desert pavement (reg)	82.15	83.92	83.93	1.77	0.01	1.78	
Volcanic plains	64.10	66.62	66.79	2.52	0.17	2.69	
High altitude alluvial fans	62.25	66.43	66.68	4.18	0.25	4.43	
Granite weathered outcrops	108.60	109.72	109.64	1.12	-0.09	1.04	
Alluvial fans with rill erosion	96.79	97.15	97.12	0.36	-0.03	0.33	
Young alluvial fans (highlands)	115.84	113.38	113.56	-2.45	0.17	-2.28	
Saline lands with Nebka landforms	80.87	82.59	83.42	1.72	0.83	2.55	
Farmlands with a high-water table	72.40	72.81	73.20	0.42	0.39	0.80	
Farmlands	104.24	103.24	103.14	-1.01	-0.1	-1.11	
Farmed claypan	108.38	105.63	105.30	-2.76	-0.33	-3.08	
Eroded lands with a high-water table	100.71	99.31	101.47	-1.40	2.15	0.75	
Non-vegetated fluvial terraces	96.35	94.52	94.77	-1.84	0.26	-1.58	
Non-vegetated regs	143.01	139.50	140.25	-3.51	0.75	-2.76	
Non-vegetated claypan	106.16	106.96	110.83	0.80	3.87	4.67	
Swamps and wetlands	67.75	69.68	71.85	1.93	2.18	4.10	
Sparsely vegetated swamps	70.48	70.65	70.99	0.17	0.34	0.52	
Fine-grained reg with rangeland cover	108.30	108.33	108.60	0.03	0.27	0.30	
Floodplain	103.78	104.17	104.67	0.39	0.50	0.89	
Detachment zones with rangeland cover	79.69	81.56	81.65	1.87	0.09	1.96	
Lowland alluvial fans with rangeland cover	122.66	121.41	121.68	-1.25	0.28	-0.98	
Saline floodplains	66.83	70.51	70.62	3.69	0.10	3.79	

in runoff production due to surface retention potential.

Runoff potential was classified into five categories from I to V (0-100% runoff production potential), indicating a range of low to very high runoff production potential. Classifying runoff generation potential in the region shows that the amount of runoff significantly increases under land-use changes. In particular, class II and III of runoff potential decreased from 1987 to 2017, while classes IV and V experienced expansion. Moreover, class V disappeared in 1989. Assuming no climatic changes, this trend would hold until 2047 in which the amount of runoff would increase due to LU/LC changes (Figure 6).

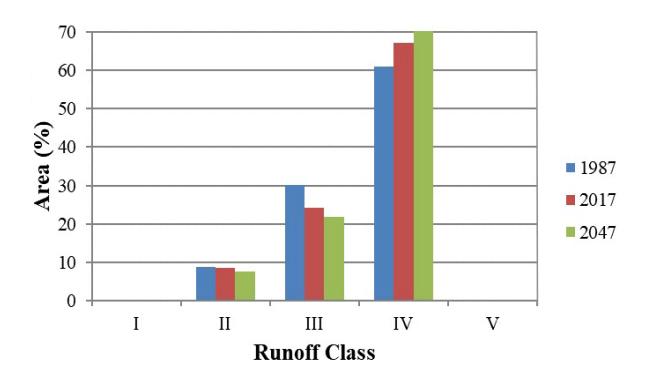


**Figure 6)** Changes in runoff classes during 1987-2047 in the Jiroft Watershed.

### **Discussion**

We used the CA-Markov methodology to evaluate and predict LU/LC and the resulting changes in CN values in the Jiroft area of Kerman Province. Based on our findings, the greatest land-use changes during the 30 years (1987-2017) of study occurred in the cases of agricultural lands, orchards, residential areas, and saline lands (i.e., 1.46%, 0.88%, 0.33%, and 7.21% increase from 1987 to 2017). In our field visits, we noticed considerable vegetation degradation in these areas. Given that the population of the area has almost increased by 38%, changes in land-use classes are of no surprise [30]. Our results proved a significant growth in runoff

class IV during the study period. Higher runoff generation due to degradation of land resources can manifest itself through the loss or deterioration of the quality of water resources, especially the surface and groundwater resources due to the changes in canopy interception, infiltration, evapotranspiration, and groundwater recharge [3].

Land-use change projection for 2047 indicated a significant increase in saline lands, residential areas, and orchards at the expense of rangelands (-2.94 for a good condition; -3.64% for moderate rangelands; -3.94% for poor rangelands). Salehi et al. [31] also projected similar results in their landuse projections. These changes will directly influence the ecological services and people's wellbeing [4], which can per se further degrade the area and increase CN values. Degradation of rangelands can affect livestock production and other side-uses of the local lands to the people. On the other hand, the expansion of saline lands and residential areas can adversely affect the agriculture sector of the region.

We found a considerable increase in CN values in the northwestern section of the region, especially due to the conversion of rangelands into less favorable land covers and saline lands. The expansion of the saline lands in the area might be attributed to the depletion of freshwater resources and the follow-up rise in the saline groundwater table, such as Jafari et al. [31] in Gorgan Province of Iran. Any increase in CN values indicates larger amounts of runoff and higher chances of flash floods in the future which agrees with Hu et al. [35], Ngo et al. [36]. In this research, we did not consider the role of climate change in future changes of runoff potential classes. Even if Iran is generally going to face a dryer state in the future, precipitation will tend to be short and intense rainfalls [37]. This is true that currently, flash floods are not much of a concern, but in the future, the LU/LC chang-

es will lead to the generation of considerable amounts of runoff and hence damages to human properties and lives. Therefore, more caution must be exercised to plan land-uses to avoid any unwanted consequences in the future. Preventing rangeland degradation, expansion of saline lands through improved drainage canals, improved agricultural practices, and improved urban and rural expansion planning could mitigate LU/LC changes [10, 33, 34].

#### Conclusion

In this research, we used a combination of RS and GIS methods to evaluate land-use changes in the Jiroft area of Iran. This region is climatically dry with scarce precipitation. However, high-intensity rainfalls could potentially induce flash floods in the area. We projected the LU/LC for the next 23 years using the CA-Markov model. We found a considerable increase in runoff potential as a result of land-use conversions and vegetation cover degradation. The greatest increase in runoff depth was obtained for the dunes (+5.83 mm) and bare lands (+4.67 mm), while alluvial plains (-4.35 mm) had the greatest reduction. We also found a 3.4% in the area of high runoff producing areas. A great percentage of the low (2%) and moderate runoff producing areas (8%) (classes II and III) will convert to the high class in 2047 (Refer to Figure 6). Most of the increase in runoff potential will occur in the western and southern sections of the study area (Figure 5). The same trend is naturally visible in Figure 4 for the CN values. The main reason behind this increase in CN and runoff potential is, in fact, land-use degradation in the area in favor of more runoff-producing ones, especially saline lands and residential areas. Our results also indicated a lower retention potential in 2047 (Figure 4) which is explained by converting rangelands into less vegetated land-uses such as impervious residential areas or bare saline lands. Even though the land-use map was validated against actual data from 100 points in 2017, we do not have any way to verify the findings for the year 2047. It might undermine the accuracy of our results. The same also holds for the runoff potential. Nevertheless, uncertainty is a part of any projection endeavor, and hence we could rely on the findings of this research given that it has produced accurate results during the validation phase. However, more effort is needed to combine the results of climate change models into runoff generation results to more accurately predict runoff which could be part of our future research. The results of this study could help land managers to utilize available water resources and prepare for any future alterations in water sources in the area.

The main findings of this research can be briefed as: a) The most significant land-use changes during the 30 years (1987-2017) of study occurred in croplands, orchards, residential areas, and saline lands; b) There is a considerable increase in CN values, especially in the northwestern section of the region, due to the conversion of rangelands into less favorable land covers and saline lands; c) We found that runoff generation has increased and will continue to increase; d) The greatest increase in runoff depth was obtained for the dunes (+5.83 mm) and bare lands (+4.67 mm) while alluvial plains (-4.35 mm) had the most significant reduction; e) The majority of areas with low runoff production had propensity of converting to classes with higher runoff production potentials; f) Land's retention capacity will decrease in the future as the response to the expansion of impervious areas and barren lands; g) Therefore, conversely to the current situation, smaller amounts of precipitation will turn into flash floods in the Jiroft Watershed in the future.

### Acknowledgments

We cordially thank the University of Kashan

for its financial support for conducting this research and the reviewers for their comments which improves the quality of the work to a great extent. We would also like to thank the Editor of the journal of Earth Science Informatics for all the efforts in preparing this research for publication.

**Ethical Permission:** The authors confirm that the research is conducted in line with all University, legal and ethical standards.

Authors' contributions: All authors contributed to the study's conception and design. Material preparation, data collection, and analysis were performed by N. N. Kalayni, A. R, Fordoei, F. Panahi, and H. Musavi. N. N. Kalayni wrote the first draft of the manuscript, and all authors commented on previous versions of the manuscript. All authors read and approved the final manuscript.

# **Conflicts of interest/Competing interests:**

The authors have no conflicts of interest to declare that they are relevant to the content of this article.

**Funding:** The University of Kashan funded this research.

### References

- 1. Jayasree V., Venkatesh B. Evaluating the hydrological response to land cover change: Dasanakatte catchment of Varahi River, Western Ghats, Karnataka. Int. J. Water Resour. Environ. Manage. 2012;3(1):23-32.
- Zhang F., Tiyip T., Feng Z., Kung H.T., Johnson V., Ding J., Tashpolat N., Sawut M., Gui D. Spatio-temporal patterns of land use/cover changes over the past 20 years in the middle reaches of the Tarim River, Xinjiang, China. Land Degrad. Dev. 2015;26(3):284-99.
- 3. Baker T.J., Miller S.N. Using the Soil and Water Assessment Tool (SWAT) to assess land use impact on water resources in an East African watershed. J. Hydrol. 2013;486(1):100-111.
- 4. de Oliveira Barros K., Ribeiro C.A.A.S., Marcatti G.E., Lorenzon A.S., de Castro N.L.M., Domingues G.F., de Carvalho J.R., Dos Santos A.R. Markov chains and cellular automata to predict environments subject to desertification. J. Environ. Manage. 2018;225(1):160-167.
- 5. Yang X., Ren L., Liu Y., Jiao D., Jiang S. Hydrological response to land use and land cover changes in a

- sub-watershed of West Liaohe River Basin, China. J. Arid Land. 2014;6(6):678-689.
- 6. Romulus C., Iulia F., Ema C. Assessment of surface runoff depth changes in Sărăţel River basin, Romania using GIS techniques. Cent. Eur. J. Geosci. 2014;6(3):363-372.
- 7. Scheffler R., Neill C., Krusche A.V., Elsenbeer H. Soil hydraulic response to land-use change associated with the recent soybean expansion at the Amazon agricultural frontier. Agric. Ecosyst. Environ. 2011;144(1):281-289.
- 8. Ladisa G., Todorovic M., Liuzzi G.T. A GIS-based approach for desertification risk assessment in Apulia region, SE Italy. Phys. Chem. Earth, 2012;49(1):103-113.
- 9. Wijitkosum S. The impact of land use and spatial changes on desertification risk in degraded areas in Thailand. Sustain. Environ. Res. 2016;26(2):84-92.
- 10. Yousefi M., Mikaniki J., Ashrafi A., Neysani Samani N. Land-use Change Detection and Modeling, Using Remote Sensing data, Markov Chains and Cellular Automata (Case Study: City of Bojnord). Geogr. Plann. Space 2018;7(26):1-16.
- 11. Ranzi R., Le T.H., Rulli M.C. A RUSLE approach to model suspended sediment load in the Lo River (Vietnam): Effects of reservoirs and land-use changes. J. Hydrol. 2012;422-423(1):17-29.
- 12. Huang T.C., Lo K.F.A. Effects of land-use change on sediment and water yields in Yang Ming Shan National Park, Taiwan. Environments 2015;2(1):32-42
- 13. Hong N.M., Chu H. J., Lin Y. P., Deng D. P. Effects of land cover changes induced by large physical disturbances on hydrological responses in Central Taiwan. Environ. Monit. Assess. 2010;166(1-4):503-520.
- 14. Halder A., Ghosh A., Ghosh S. Supervised and unsupervised landuse map generation from remotely sensed images using ant based systems. Appl. Soft Comput. 2011;11(8):5770-5781.
- 15. Veldkamp A., Lambin E.F. Predicting land-use change. Agric. Ecosyst. Environ. 2001;85(1-3):1-6.
- 16. Keshtkar H., Voigt W. A spatiotemporal analysis of landscape change using an integrated Markov chain and cellular automata models. Model. Earth Syst. Environ. 2016;2(10):1-13.
- 17. Rimal B., Zhang L., Keshtkar H., Haack B.N., Rijal S., Zhang P. Land use/land cover dynamics and modeling of urban land expansion by the integration of cellular automata and Markov chain. ISPRS Int. Geo-Inf. 2018;7(4):1-21.
- 18. Torrens P.M., O'Sullivan D. Cellular automata and urban simulation: where do we go from here?: SAGE Publications Sage UK: London, England. 2001;28(2):163-168.
- 19. Ding H.p., Chen J.p., Wang G.w., editors. A mod-

el for desertification evolution employing GIS with cellular automata. 2009 International Conference on Computer Modeling and Simulation; 2009 Feb. 20 2009 to Feb. 22 2009; Macau: IEEE.

- 20. Ghaderi S., Zare Chahouki M., Azarnivand H., Tavili A., Raygani B. Land-use Change Prediction using CA-Markov modeling (Case Study: Eshtehard). Rangeland 2020;14(1):147-160.
- 21. Yousefi S., Mirzaee S., Tazeh M., Pourghasemi H., Karimi H. Comparison of different algorithms for land use mapping in dry climate using satellite images: a case study of the Central regions of Iran. Desert 2015;20(1):1-10.
- 22. Firozjaei M.K., Kiavarz M., Alavipanah S.K., Lakes T., Qureshi S. Monitoring and forecasting heat island intensity through multi-temporal image analysis and cellular automata-Markov chain modelling: A case of Babol city, Iran. Ecol. Indic. 2018;91(1):155-70.
- 23. Cronshey R., Roberts R., Miller N., editors. Urban hydrology for small watersheds (TR-55 Rev.). Hydraulics and Hydrology in the Small Computer Age; 1985 August 12-17, 1985; Lake Buena Vista, Florida, United States ASCE.
- 24. Satheeshkumar S., Venkateswaran S., Kannan R. Rainfall-runoff estimation using SCS–CN and GIS approach in the Pappiredipatti watershed of the Vaniyar sub-basin, South India. Model. Earth Syst. Environ. 2017;3(1):1-9.

- 25. Naboureh A., Moghaddam M.H.R., Feizizadeh B., Blaschke T. An integrated object-based image analysis and CA-Markov model approach for modeling land use/land cover trends in the Sarab plain. Arab. J. Geosci. 2017;10(12):1-16.
- 26. Mosayebi M., Maleki M. Change detection in land use using remote sensing data and GIS (Case study: Ardabil county). J. RS GIS Nat. Res. 2014;5(1):75-86.
- 27. Salehi N., Ekhtesasi M.R., Talebi A. Predicting locational trend of land-use changes using CA-Markov model (Case study: Safarod Ramsar watershed). J. RS GIS Nat. Res. 2019;10(1):106-120.
- 28. Jafari Shalamzari M., Zhang W., Gholami A., Zhang Z. Runoff Harvesting Site Suitability Analysis for Wildlife in Sub-Desert Regions. Water 2019;11(9):1-23.
- 29. Sheikh V.B., Jafari Shalamzari M., Farajollahi A., Fazli P. Soil erosion under simulated rainfall in loess lands with emphasis on land-use, slope and aspect. ECOPERSIA 2016;4(2):1395-1409.
- 30. Hu S., Fan Y., Zhang T. Assessing the effect of landuse change on surface runoff in a rapidly urbanized city: A case study of the central area of Beijing. Land. 2020;9(1):1-15.
- 31. Ngo T.S., Nguyen D.B., Rajendra P.S. Effect of landuse change on runoff and sediment yield in Da River Basin of Hoa Binh Province, Northwest Vietnam. J. Mt. Sci. 2015;12(4):1051-1064.